Dynamic Laser Speckle Technique as an alternative tool to determine hygroscopic capacity and specific surface area of microporous zeolites

Ruth Dary Mojica-Sepulveda[1], Luís Joaquín Mendoza-Herrera[2,3], Eduardo Grumel[2,3], Delia Beatriz Soria[1], Carmen Inés Cabello[3,4,5,*], and Marcelo Trivi[2,3,5]

[1] *Centro de Química Inorgánica (CEQUINOR), CONICET-CCT La Plata, UNLP, La Plata, Argentina.*

[2] *Centro de Investigaciones Opticas (CIOp), CONICET-CCT La Plata-UNLP-CICPBA, P.O.Box 3 (1897) Gonnet-La Plata, Argentina.*

[3] *UID Optimo, Dpto. Cs. Básicas, Facultad de Ingeniería, Universidad Nacional de La Plata (UNLP), La Plata, Argentina.*

[4] *Centro de Investigación y Desarrollo en Ciencias Aplicadas Dr. J. J. Ronco (CINDECA) CONICET- CCT La Plata, UNLP Calle 47 N 257 (1900) La Plata, Argentina.*

[5] *CICPBA, Comisión Investigaciones Científicas Provincia Buenos Aires, Argentina.*

[*] *Corresponding author: ccabello@quimica.unlp.edu.ar*

Abstract

Adsorption phenomena have several technological applications such as desiccants, catalysts, separation of gases, etc. Their uses depend on the textural properties of the solid adsorbent and the type of the adsorbed liquid or gas. Therefore, it is important to determine these properties. The most common measurement methods are physicochemical based on adsorption of N_2 to determine the surface area and the distribution of pores size. However these techniques present certain limitations for microporous materials. In this paper we propose the use of the Dynamic Laser Speckle (DLS) technique to measure the hygroscopic capacity of a microporous natural zeolite and their modified forms. This new approach based on the adsorption of water by solids allows determine their specific surface area (S). To test the DLS results, we compared the obtained S values to those calculated by different conventional isotherms using the N_2 adsorption-desorption method.

keyword: Dinamic laser speckle; nitrogen physisorption; specific surface area; BET

I. INTRODUCTION

The minerals based on aluminosilicates (AS) such as zeolites (clinoptilolite) and clays (kaolinite, montmorillonite) are abundant and inexpensive [1]. Zeolites and kaolinites are two relevant examples of natural AS. Due to their physicochemical properties, nontoxicity, low cost, and easy availability, these materials are important in geology, agriculture, catalysis, industrial (ceramics, paper, paint, etc.) and environmental processes [2–6].

When an AS is "activated" by a thermal treatment, an dehydration process occurs and they acquire a great adsorption capacity. Additionally, the treatment with concentrated acids or bases also modifies their hygroscopic properties as previously reported [7–9]. Furthermore is renowned that hydrogen bonding interactions and electrostatic attraction forces on the surface of AS modified with anionic and/or cationic species has a significant effect on different industrial application [3, 4].

The most validated and accepted procedure by international standards for the determination of the pore size distribution and specific surface area of different porous materials is nitrogen physisorption and numerous isotherms have been used to describe this processes. One the first reported studies of the adsorption nitrogen and other gases was the Langmuir isotherm model [10], however Brunauer, Emmett and Teller (BET) Isotherm [11, 12] is the most used. The BET-nitrogen model is established as an ISO standard procedure for surface area determination in spite of the perceived theoretical limitations. One of the inherent difficulties, is to consider the energetic homogeneity for all adsorption sites on the surface and so an inadequate fit of the experimental data at low pressure region is applied [13].

Futhermore, the BET model is based in the slighlty consideration about the interactions forces between the adsorbent and the adsorbate molecules. For all these limitations in the BET model, Chirife [14–18] and Henderson [19] isotherms are widely used for this purpose.

In our knowledgment, no other suitable alternative method has been reported for the characterization of specific area. For that reason should be necessary to have a simple and non-destructive method to study the surface properties of different materials specially aluminosilicates. In this paper we propose a method using a dynamic laser speckle (DLS) technique.

DLS is a versatile technique used for different applications, such as determination of very small surfaces displacements and rotations, the viability of a seed, the drying time of paints and several biologic and biomedical applications [20–27]. This simple and relatively inexpensive technique can be also used for the hygroscopic characterization of different materials. We have previously reported the hygroscopic study of the zeolites modified with acid, base and temperature treatment by using the dynamic laser speckle technique [9]. In view of the foregoing results obtained by the DLS as a characterization technique for zeolites, we herein report a useful and alternative method for the specific surface area determination

II. EXPERIMENTAL

Zeolite Clinoptilolite is a mineral from La Rioja, Argentine. The natural sample was modified by 1M solutions of ammonium hydroxide and nitric acid and they were also thermally treated at 250°C (523.15 K) and 500°C (773.15 K). For more details see [9]. Surface areas and porosity of samples were determined by physical N_2 adsorption at 77 K (BET model) using a Micromeritics apparatus ASAP 2010.

Dynamic laser speckle (DLS) is an optical technique that has been used for various applications in biology, medicine and industry [20]. It is based on a scattering phenomenon that occurs when a coherent laser light illuminates an active surface. The surface seems to be covered by tiny bright and dark spots that fluctuate in an apparently random fashion, according to the fluctuation of the surface.Therefore, the study of the temporal evolution of speckle patterns can provide an interesting tool to characterize the parameters involved in the dynamic processes of the sample.

We use the DLS technique to measure the hydroadsorption process of the zeolite. In this case, 30 mg of each sample were impregnated with 10μl distilled water and the experiment was carried out at 19°C (292.15 K) and 60% of humidity. Figure 1 shows the experimental DLS set-up. We employ a 10 mW He-Ne laser to illuminate the samples and a CCD camera connected to a frame grabber to record and digitize the speckle patterns images. Then, we construct a Temporal History of Speckle Pattern (THSP) matrix (see Fig. 2) and follow the Oulamara et al. [28] method. The activity of the sample appears as intensity changes in the horizontal direction. For example, when the sample is very active (initial hydro-adsorption process), THSP looks like a speckle pattern (See Figure 2a). When the sample have low

activity (process complete), THSP shows elongated shapes(See Figure 2b).

Finally, we use the Arizaga et. al [29] method to process the THSP data. We calculate the second order moment of the Co-occurrence matrix for quantitative measurements.

$$MSO = \sum_{ij} M_{ij} \, (i-j)^2 \tag{1}$$

where M_{ij} is the number of the gray-level i followed by the gray level j in the horizontal direction of the THSP matrix. For more details of this method see References [9] and [29].

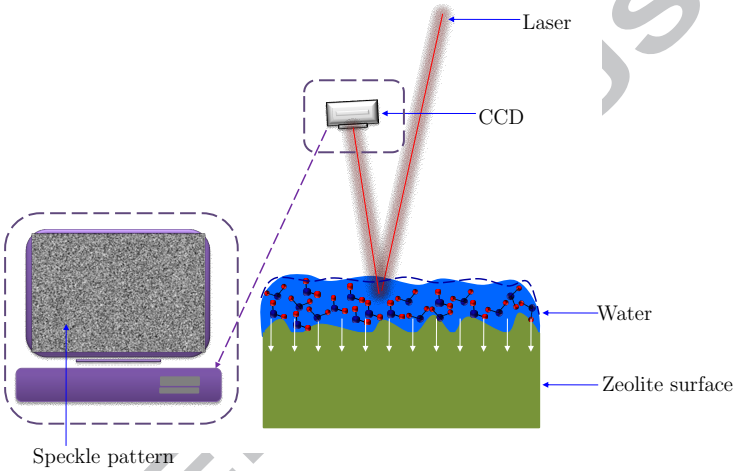

FIG. 1. Scheme of the experimental set up used for the dynamic speckle technique. The dotted curves represent the temporaly progress of water adsorption.

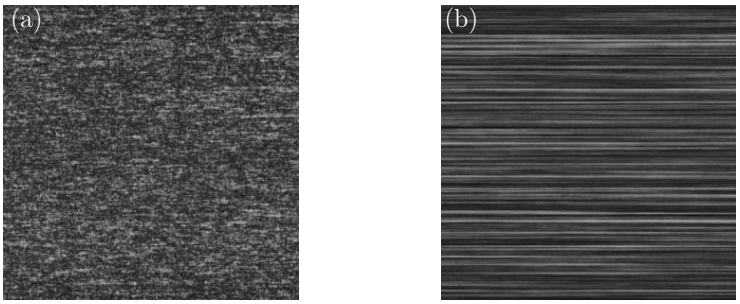

FIG. 2. Temporal History of Speckle Pattern, (a) high activity (initial hydro-adsorption process), (b) low activity (process is complete).

III. SORPTION ISOTHERMS

Different isotherms describing the adsorption-desorption processes in different pressure ranges [14–19, 30–39] are show in Table 1.

TABLE I. Different models of isotherms usefull to reproduce a sorption process in a solid.

Isotherm	Expression
Langmuir [30]	$Q_A = Q_m \frac{bP}{1+bP}$
Freundlich [30]	$Q_A = KP^{1/n}$
Tenkim [30]	$Q_A = A \log(BP)$
Brunauer, Emmett and Teller (BET) [30–33]	$\frac{P}{Q_A(1-P)} = \frac{1}{Q_m C} + \frac{C-1}{Q_m C} P$
Guggenheim, Anderson, and Boer (GAB) [30–33]	$\frac{k_G P}{Q_A(1-k_G P)} = \frac{1}{Q_G C_G} + \frac{C_G - 1}{Q_G C_G} k_G P$
Three stage sorption model (t.s.s.) [32]	$\frac{k_t P}{Q_A(1-k_t P)} = \frac{1}{Q_t C_t H H'} + \frac{C_t H - 1}{Q_t C_t H H'} k_t P$ $H = 1 + \frac{(k_t P)^h}{1-P} \frac{1-k_t}{k_t}$ $H' = 1 + \frac{H-1}{H} \frac{1-k_t P}{1-P} [P - h(1-P)]$
Three stage sorption restricted model (t.s.s.r.) [32, 33]	$\frac{k_t r P}{Q_A(1-k_t r P)} = \frac{1}{Q_t r C_t r G G'} + \frac{C_t r G - 1}{Q_t r C_t r G G''} k_t r P$ $G = H - \frac{1}{k_t r} \frac{1-k_t r P}{1-P} \frac{1-k_t}{k_t}$ $G' = \frac{H-1}{G} - \frac{1-k_t r P}{1-P} Q$ $Q = P + h(1-P) - \left[P - (1-P)(1-k_t r P) \frac{h+n}{1-f}\right] P^n$
Oswin [34]	$Q_A = K \left(\frac{P}{1+P}\right)^n$
Chirife [14–18]	$Q_A = K \left(\frac{-A}{\log P}\right)^{1/C}$
Ferro-Fontain [35]	$\log\left(\frac{\gamma}{Q_A}\right) = \alpha P^r$
Lewicki [36]	$Q_A = A \left(\frac{1}{P-1}\right)^{b-1}$
Henderson [19]	$Q_A = K \left(-A \log(1-P)\right)^{1/C}$
Chung-Pfost [37, 38]	$Q_A = \frac{\log \frac{\log P}{-A}}{-B}$
Viollaz [39]	$Q_A = \frac{Q_V C_V k_V P}{(1-k_V P)(1+(C_V-1)k_V P)} + \frac{Q_V k_V k_2}{(1-k_V P)(1-P)}$

Where Q_A is the adsorbed N_2 amount and P is the relative pressure. The other parameters are constants and is necessary to be calculated.

The water adsorption by the zeolite is a process that can be studied using these models.

Furthermore, as previously reported in Reference [9], Hawkes and Flink, Peleg and Azuara models can be also used [40–50]. Application of all these models to the DLS experimental data resulted in a not good fit. In Ref [9] the Peleg equation was modified extending it to the second order. Although a better adjustment was achieved, this equation does not show the entire adsorption process. Therefore, we propose a new model that takes into account all the dynamics of the water adsorption process.

IV. PROPOSED MODEL FOR DLS IN ZEOLITE SAMPLES

One empirical approach involves the consideration of the solid zeolite with cylindrical pores with R as a mean radius, $L(t)$ as average depth and $H(t)$ indicates the height of water in all surface occupied. These values changes with the hydration. According to this, the Hagen-Poiseuille's law can be used to calculate the water flow, Q_A

$$Q_A = \frac{\rho g H \pi R^4}{8\eta L} = \frac{dV}{dt} \tag{2}$$

Where V is the water volume, ρ and η are the water density and viscosity, respectively. The water volume variation due to the hydration is described as $\pi R^2 dh(t)/dt$, where $h(t)$ is the water height in the pore. Using these considerations in equation (1), the height of water in the pore can be calculated.

$$\frac{dh(t)}{dt} = \frac{\rho g H \pi R^2}{8\eta} \frac{H_0 - h(t)}{L_0 - h(t)} \tag{3}$$

The solution of this equation with the appropriate initial conditions (L_0 and H_0) is:

$$A \ln(U) - U - A \ln H_0 + H_0 = Ct \tag{4}$$

where $U = H_0 - h(t)$, $C = \frac{\rho g R^2}{8\eta}$, $A = H_0 - L_0$.

With the aim to reproduce the experimental data of the second order moment (MSO) must be taking into account their proportionality to the remain water height ($MSO \propto U = H_0 - h(t)$)

V. RESULTS AND DISCUSSION

A. Determination of specific surface area (S)

Figures 3a) and 3b) display the different isotherms models describing nitrogen adsorption-desorption isotherms at 77 K in the natural zeolite. The best fit with the experimental data was observed for the Chirife's isothermal model (continuous black line in figure 3.b, with values A = -9.7033 and C = 2.3487). However, as observed in Figure 3, the fitting of the two isotherm models Ferro-Fontain (green segments and points in Figure 3.b) and Villoaz (short and long fuchsias segments in Figure 3.b) is not good.

TABLE II. Summary of the different isotherms models and their parameters calculated.

Pressure range	Isotherm	Parameters
0.01-0.93	t.s.s	Q_t = 1.7667, C_t = 278.91, h = 27.9 and k_t = 0.81
0.01-0.90	t.s.s.r	Q_{tr} = 1.7664, C_{tr} = 265.83, k_{tr} = 0.80, h = 16.9, n = 0.10 and f = 0.05
0.01-0.82	GAB	k_G = -101.6484, C_G = 1.0071 and Q_G = -1.9841
0.01-0.60	Chung-Fost	A = 19.1245 and B = 1.1055
0.01-0.45	Lewicki and Oswin	N = 0.1851 and K = 2.9179 A = 2.9179 and b = -0.1851
0.01-0.35	BET	Q_m = 1; 8472 and C = 134.11.
0.01-0.30	Freundlich	K = 2.9449 and n = 5.4282
	Henderson	A = 0.0284 and C = 2.1926
0.01-0.25	Temkin	A = 0.3209 and B = 4215.1
0.01-0.10	Langmuir	Q_m = 1.9481 and b = 139.7382

Table 2 shows the parameters calculated by using isotherms models in different pressure range.

The Chirife isotherm model was applied to the natural and modified zeolites due to the good results obtained by this model. Figure 4 shows the experimental values of the N_2

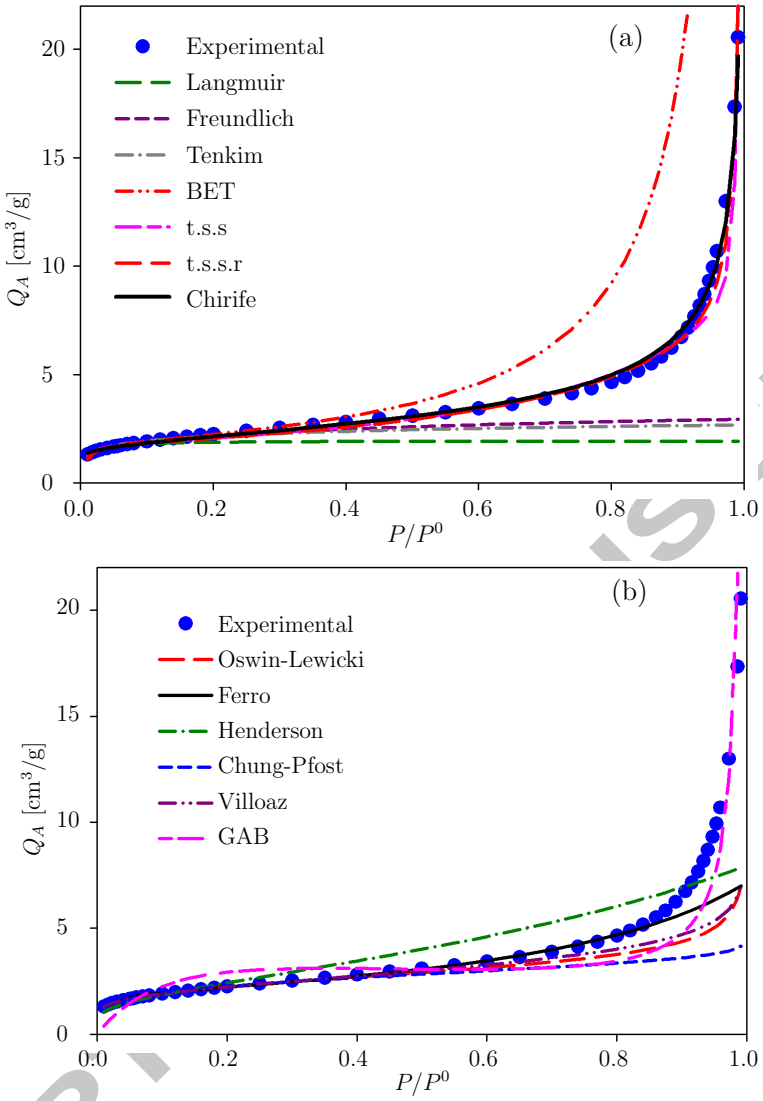

FIG. 3. Experimental values of N_2 sorption in blue dots and the theoretical adjustments (a) Langmuir, Freundlich, Tenkim, BET, t.s.s, t.s.s.r and Chirife (b) Oswin-Lewicki, GAB, Ferre-Fountain, Henderson, Chung-Pfost and Villoaz.

sorption for all the samples and the respective adjustments with the Chirife's isotherm. As observed in Figure 4 the different curves do not show important differences in the experimental values for samples.

Using this model the specific surface area for all samples were calculated and the values are summarized in Table 3 which also includes those obtained by BET model

Halsey [51], Harkins and Jura [52], and Harkins and Jura modified by Kruk [53] are used in the corresponding t-plots for determining the external area for all samples (2.5Å-5.0 Å).

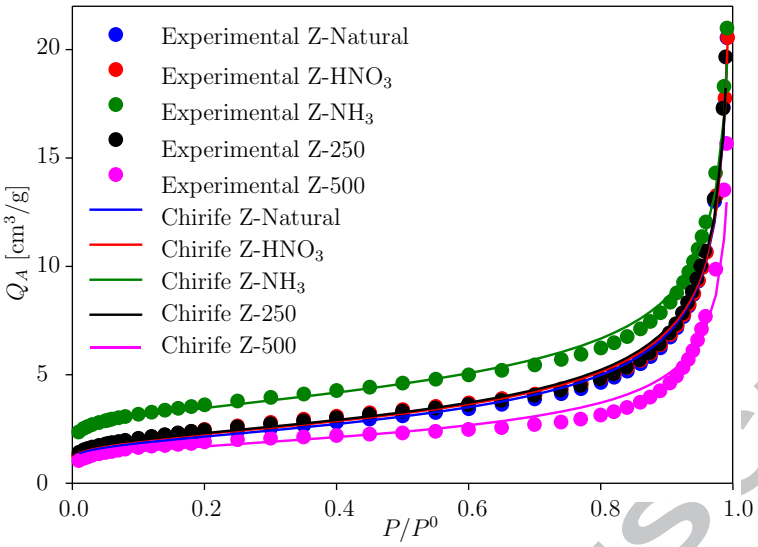

FIG. 4. Experimental values of the N_2 sorption for the natural zeolite and its chemical and thermal modification derivatives, and the respective adjustments with the Chirife isotherm.

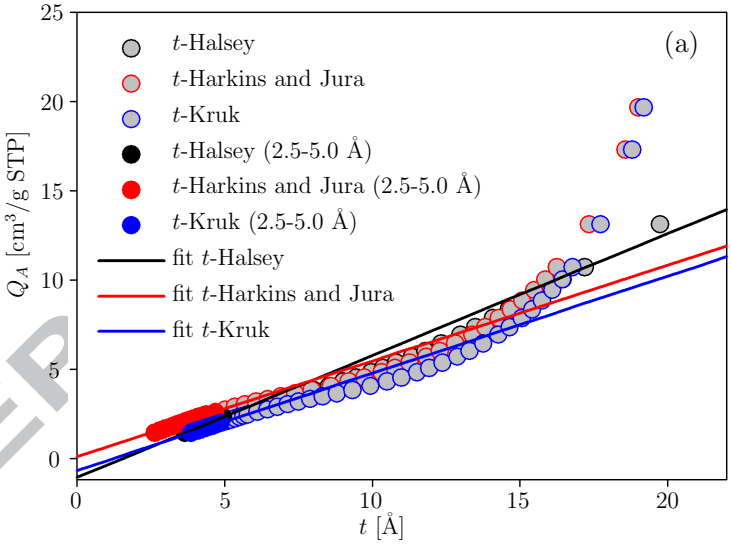

FIG. 5. t-plots of Hasley, Harkins and Jura and Harkins and Jura modified by Kruk models.

Figure 5 shows the t-plot for the natural zeolite even was determined for all samples (see Figure A9-A12). As can be observed in the Figure 5 the Halsey and Kruk equations result in negative values for Q_A giving rise to negative volume of micropores whith does not have any real physical meaning. For that reason the Harkins and Jura model was applied to calculate the external area and the volume of the micropores. The results for all samples are also included in Table 3. The effective surface area for the BET model determined for natural

and Z-250 samples is lower than that for the external area and this result has no sense. However, this contradiction is not observed with Chirife isotherm, as observed in Table 3.

TABLE III. Specific and external surface area S, volume of micropores and energy D-R (Dubinin-Radushkevich) for all samples.

Sample	$S_{Chirife}$	S_{BET}	$S_{ext.}$	V_{micro}	V_{micro}	E(kJ)
	$[m^2/g]$	$[m^2/g]$	$[m^2/g]$		D-R	
Natural	11.4552[2023]	6.7951[0314]	7.4501	0.218	0.206	6.4
Z-HNO_3	11.9325[2574]	8.0412[0431]	5.6949	0.432	0.219	6.0
Z-NH_3	12.2367[2368]	8.7585[0574]	8.2914	0.155	0.337	7.3
Z-250	13.7170[2435]	8.8600[0914]	9.6264	0.000	0.181	5.9
Z-500	17.6741[2715]	12.7963[0292]	9.4980	1.421	0.222	6.5

It is very known that the Dubinin-Radushkevich model is very useful to calculate the total volume of micropores and the characteristic energy of the fluid-solid system. With the aim to have a complete information about the morphology of the porous materials, the knowing of the size pores distribution is neccesary. Barrett, Joyner and Halenda (BJH) [54] is the most accepted method for determining the size of mesopores.

However, previously report, indicate that the BJH method overestimate the pore size [55]. The authors proposed an improved method, named VBS, where they use the adsorption-desorption isotherm reconstruction. This method include a corrective factor (f_c) to the standard BJH equation, whose value is selected to satisfy a criterion of its own consistency, ie, the reconstructed isotherm must adjusted to the original.

Finally, for all samples the f_c values determined from VBS method, for desorption are 0.08, 0.17, 0.00, 0.10 and 0.02 for Z-Natural, Z-250, Z-500, Z-NH_3 and Z-HNO_3 respectively. Figure 6 shows the pore distributions for different zeolite samples. It can be observed that Z-HNO_3 presents the most important differences, while the smallest differences are found for Z-NH_3. It is noted that the width of pores mostly varies between 2 and 10 nm indicating that these samples have supermicropores and mesopores according to IUPAC.

After determining the specific surface area by using the nitrogen physisorption technique (using the Chirife isotherm which is most appropriate to describe all samples), the characteristic time of water adsorption must be determined using DLS technique.

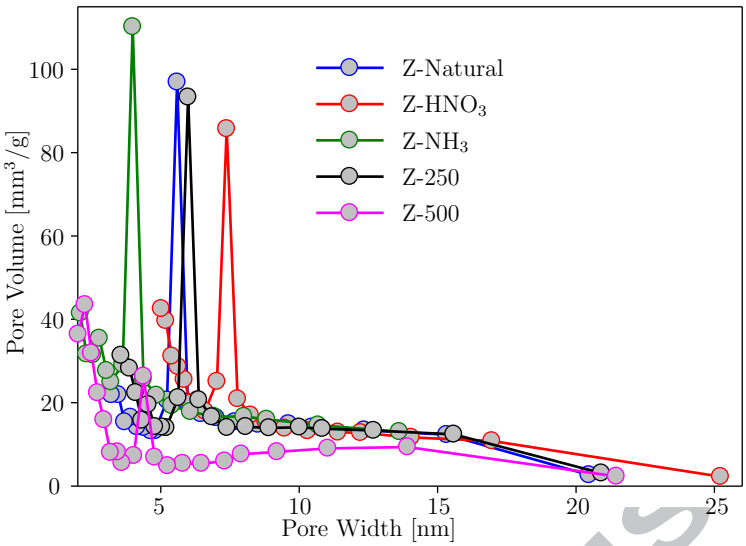

FIG. 6. Pores size distribution of all samples.

B. Determination of the characteristic time for the water adsorption

Figure 7 shows the second order moment for the experimental values of natural zeolite samples and those determining using different conventional isotherms were plotted as a funtion on time. Fig A13-A16 show the results for the other samples

As shown in Figure 7 any models not fit very well, except for that calculated using the new propose model (See equation (3). Figure 7b shows the good agreement between the experimental value and the proposed model (continuous blue line). This model predicts the "characteristic time" (τ) which is considered as the instant in which the second order moment reaches 37% of its initial value.

In Table 4 are summarized the characteristic times for all samples calculated with our proposed model.

C. Calibration Curve

Taking into account the good results obtained with our model, it would be very useful for determining the specific surface area. For this purpose it is necessary to have a calibration curve.

Figure 8 shows the linear regression between specific surface area [$S(\mathrm{m}^2/\mathrm{g})$] (Chirife and

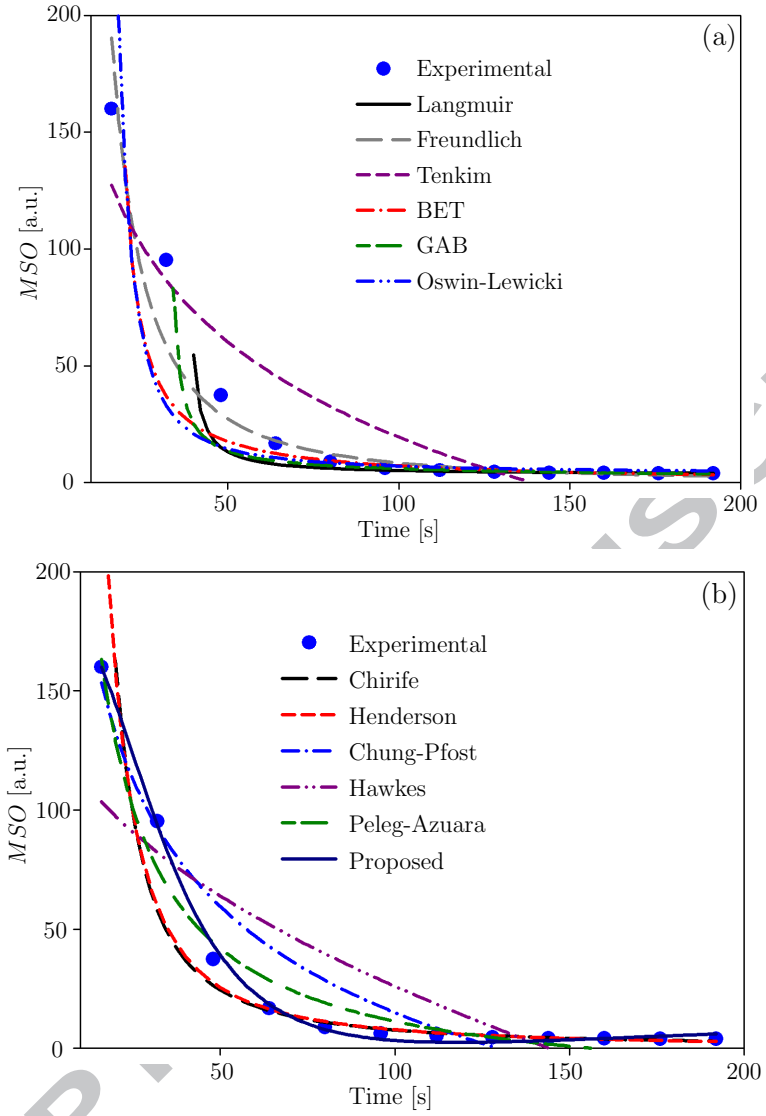

FIG. 7. Experimental values of the second order moment as a function of time and isotherm values adjusted by the different models for water adsorption of the natural zeolite. DLS technique values in blue dots.

BET) and characteristic time [τ] for all samples. From these Figures it is possible to obtain the following equations:

Using Chirife isotherm model:

$$S_{Chirife} = 0.0453\tau + 10.1874 \tag{5}$$

Using BET isotherm model:

TABLE IV. Characteristic time of natural and modified zeolites calculated with our proposed model

Zeolite	τ[s]
Natural	25.830
Z-HNO_3	31.048
Z-NH_3	50.294
Z-250	87.561
Z-500	160.221

$$S_{BET} = 0.0390\tau + 6.2839 \tag{6}$$

These equations are a simple and a very useful method to determine the specific area with the water adsorption DLS calculated characteristic time from Chirife and BET's isotherms models.

As observed in Table 4 the values of the DLS characteristic time determined for all samples with our model, are very different between them while those for the specific area are very similar (see Table 3).

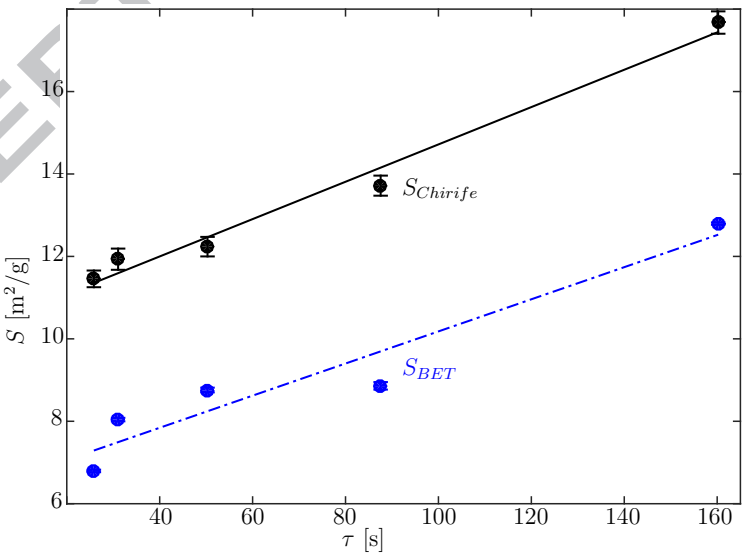

FIG. 8. Specific surface area vs. characteristic time (τ)

VI. CONCLUSIONS

In this paper, we propose a new approach to study hydroadsorption properties of solids materials using a simple and non destructive method named Dynamic Laser Speckle (DLS). It was also possible to determine the specific surface area of different samples. As examples of this proposal, we studied several pure and modified clinoptilolite samples.

A careful analysis was carried out about the textural properties of all samples (porosity, specific surface and external area) by the N_2 adsorption method. For this purpose, several known isotherms were applied. The pore size was estimated by the BJH model. In addition, we applied the VBS model for determining the f_c parameter using a matlab algorithm. This parameter was used to correct the overestimation predicted by the BJH model in the pore size. Finally, using the Dubinin-Radushkevich model, we determined the volume of the micropores.

Through this analysis, we demonstrate that Chirife's isotherms models fitting better than the BET traditional model to describe the experimental value of the N_2 sorption of all the studied samples.

We propose a new model for determining the "characteristic time" (τ) of the water adsorption process using the experimental value from the second order moment of DLS method. Then, we compared the specific surface areas obtained by DLS with those obtained by the conventional N_2 adsorption methods.

The conventional sorption methods are quite complicated to use because they its need reagents in expensive equipment with high vacuum and data processing require careful mathematical treatment to adjust the isotherms that characterize the textural properties of the adsorbents.

On the other hand, for our proposal it is sufficient to illuminate a small amount of a controlled moistened sample with a low cost laser instrument. Then the acquisition and processing of experimental data is done in a simple way using a standard mathematical model.

Then, DLS could be considered as a potential low cost, non-destructive and simple method to characterize adsorption materials for different applications.

REFERENCES

[1] V.J. Inglezakis, V.J. Stylianou, and M. Loizidou. Ion exchange and adsorption equilibrium studies on clinoptilolite, bentonite and vermiculite. *Journal of Physical Chemistry A*, 71:279–284, 2010.

[2] A. Rivera and T. Farias. Clinoptilolite-surfactant composites as drug support: A new potential application. *Microporous and Mesoprous Materials*, 80:337–346, 2005.

[3] M. Panagiotis. Application of natural zeolites in environmental remediation: A short review. *Microporous and Mesoprous Materials*, 144:15–18, 2011.

[4] K. Palevic, B. Subotic, and M. Colic. Studies in surface science and catalysis. In Galarneau A., Di Renzo F., Fagula F., and Vedrine J., editors, *Zeolites and Mesoporous Materials at the Dawn of the 21st Century.*, volume 35, pages 32–O–01. Elsevier Science, 2001.

[5] A. Araya and A. Dyer. Studies on natural clinoptilolites. *Journal of Inorganic and Nuclear Chemistry*, 43:589–598, 1981.

[6] J. Chistopher Rhodes. Properties and applications of zeolites. *Science Progress*, 93:223–284, 2010.

[7] J.R. Goldsmith. Al/si interdiffusion in albite: Effect of pressure and the role of hydrogen. *Contributions to Mineralogy and Petrology*, 95:311–321, 1987.

[8] J.R. Goldsmith. Enhanced al/si diffusion in $KAlSi_3O_8$ at high pressures: The effect of hydrogen. *The Journal of Geology*, 96:109–124, 1988.

[9] R. D. Mojica-Sepulveda, L. J. Mendoza-Herrera, M. F. Agosto, E. Grumel, D. B. Soria, C. I. Cabello, and M. Trivi. Hydro-adsorption study by dynamic laser speckle of natural zeolite for adsorbent and fertilizer applications. *Advances in Chemical Engineering and Science*, 6:570–583, 2016.

[10] I. Langmuir. The adsorption of gases on plane surfaces of glass, mica and platinum. *Eucker Verh deut physik*, 16:345, 1918.

[11] S. Brunauer, L.S. Deming, and E. Teller. On a theory of van der waals adsorption of gases. *Journal of the American Chemical Society*, 62:1723–1732, 1940.

[12] S. Brunauer, P.H. Emmet, and E. Teller. Adsorption of gases in multimolecular layers. *Journal*

of the American Chemical Society, 60:309–319, 1938.

[13] Kenneth Sing. The use of nitrogen adsorption for the characterisation of porous materials. *Colloids and Surfaces A: Physicochemical and Engineering Aspects*, 187-188:3–9, 2001.

[14] J. Chirife and H.A. Iglesias. Equations for fitting water sorption isotherms of foods: Part i. a review. *Journal of Food Technology*, 13:159–174, 1978.

[15] H.A. Iglesias and J. Chirife. Equilibrium moisture content of air dried beef: Dependence on drying temperature. *Journal of Food Technology*, 11:567–573, 1976.

[16] H.A. Iglesias and J. Chirife. Prediction of effect of temperature on water sorption of food materials. *Journal of Food Technology*, 11:109–116, 1976.

[17] H.A. Iglesias and J. Chirife. A model for describing the water sorption behavior of foods. *Journal of Food Technology*, 41:984–992, 1976.

[18] H.A. Iglesias and J. Chirife. An alternative to the Guggenheim, Anderson and De Boer for the mathematical description of moisture sorption isotherms of foods. *Food Research International*, 28:317–321, 1995.

[19] S.M. Henderson. A basic concept of equilibrium moisture. *Agricultural Engineering*, 33:29–32, 1952.

[20] H. Rabal and R. Braga. *Dynamic Laser Speckle and Applications*. CRC Press, 1 edition, 2009.

[21] R. Arizaga, N. Cap, H. Rabal, and M. Trivi. Display of local activity using dynamical speckle patterns. *Optical Engineering*, 41:287–294, 2002.

[22] M. Pajuelo, G. Baldwin, R. Arizaga, N. Cap, H. Rabal, and M. Trivi. Bio-speckle assessment of bruising in fruits. *Optics and Lasers in Engineering*, 40:13–24, 2003.

[23] R. A. Braga, G. F. Rabelo, L. R. Granato, E. F. Santos, J. C. Machado, R. Arizaga, Héctor J. Rabal, and Marcelo Trivi. Detection of fungi in beans by the laser biospeckle technique. *Biosystems engineering*, 91:465–469, 2005.

[24] R. A. Braga, I. M. Dal Fabbro, F M Borem, G Rabelo, R Arizaga, H J Rabal, and Marcelo Trivi. Assessment of seed viability by laser speckle techniques. *Biosystems engineering*, 86:287–294, 2003.

[25] J. I. Amalvy, C. A. Lasquibar, R. Arizaga, H. Rabal, and M. Trivi. Application of dynamic speckle interferometry to the drying of coatings. *Progress in Organic Coatings*, 42:89–99, 2001.

[26] S. Joughehdoust and S. Manafi. Application of zeolite in biomedical engineering: A review. *Iran International Zeolite*, 2008.

[27] H. Rabal, R. Arizaga, N. Cap, M. Trivi, G. Romero, and E. Alanis. Transient phenomena analysis using dynamic speckle patterns. *Optical engineering*, 35:57–62, 1996.

[28] A. Oulamara, G. Tribillon, and J. Dubernoy. Biological activity measurement on botanical specimen surfaces using a temporal decorrelation effect of laser speckle. *Journal of Modern Optics*, 36:165–179, 1989.

[29] Ricardo Arizaga, Marcelo Trivi, and Héctor Rabal. Speckle time evolution characterization by the co-occurrence matrix analysis. *Optics & Laser Technology*, 235:163–169, 1999.

[30] J. H. de Boer. *The Dynamical Character of Adsorption*. Clarendon Press: Oxford, 1 edition, 1968.

[31] E. O. Timmermann. A. B. E. T.-like three sorption stage isotherm. *Journal of the Chemical Society, Faraday Transactions I: Physical Chemistry in Condensed Phases*, 85:1631–1645, 1989.

[32] E. O. Timmermann, J. Chirife, and H. A. Iglesias. Water sorption isotherms of foods and foods stuffs bet or gab parameters. *Journal of Food Engineering*, 48:19–31, 2001.

[33] E. O. Timmermann. Multilayer sorption parameters: BET or GAB values. *Colloids and Surfaces A: Physicochemical and Engineering Aspects*, 220:235–260, 2001.

[34] C. R. Oswin. The kinetics package life III. the isotherm. *Journal of Society Chemical Industry*, 65:419–421, 1946.

[35] C. Ferro-Fontan, J. Chirife, E. Sancho, and H. A. Iglesias. Analysis of a model for water sorption phenomena in foods. *Journal of Food Science*, 47:1590–1594, 1982.

[36] P. P. Lewicki. Raoult's law based food water sorption isotherm. *Journal of Food Engineering*, 43:31–40, 2000.

[37] D. S. Chung and H. B. Pfost. Adsorption and desorption of water vapour by cereal grains and their products. part i. heat and free energy changes of adsorption and desorption. *Transactions of the ASAE*, 10:549–551, 1967.

[38] D. S. Chung and H. B. Pfost. Adsorption and desorption of water vapour by cereal grains and their products. part ii. hypothesis for explaining the hysteresis effect. *Transactions of the ASAE*, 10:552–555, 1967.

[39] P. Viollaz and C. O. Rovedo. Equilibrium sorption isother and thermodynamic properties of starch and gluten. *Journal of Food Engineering*, 40:287–292, 1999.

[40] M. Peleg. An empirical model for the description of moisture sorption curves. *Journal of Food*

Science, 53:1216–1217, 1988.

[41] C. I .Beristain, E. Azuara, H. S. Garcia, and E. J. Vernon-Carter. Kinetic model for water/oil absorption of mesquite gum (prosopisjuliflora) and gum arabic (acacia senegal). *International Journal of Food Science and Technology*, 31:379–386, 1996.

[42] H. O. Agu, M. H. Badau, and U. M. Abubakar. Modeling the water absorption characteristics of various local pearl millet grains and hungry rice (digitariaexilis) during soaking using pelegs equation. *Focusing on Modern Food Industry*, 2:161–169, 2013.

[43] J. Hawkes and J. M. Flink. Osmotic concentration of fruit slices prior to freeze dehydration. *Journal of Food Processing and Preservation*, 2:265–284, 1978.

[44] E. Azuara, C. I. Beristain, and G. F. Gutiérrez. A method for continuous kinetic evaluation of osmotic dehydration. *Lebensmittel-Wissenschaft und -Technologie*, 31:317–321, 1998.

[45] E. Azuara, R. Cortes, H. S. Garcia, and C. I. Beristain. Kinetic model for osmotic dehydration and its relationship with fick's second law. *International Journal of Food Science and Technology*, 27:409–418, 1992.

[46] S. M. Shafaei, A. A. Masoumi, and H. Roshan. Analysis of water absorption of bean and chickpea during soaking using Peleg model. *Journal of the Saudi Society of Agricultural Sciences*, 15:135–144, 2016.

[47] M. Turhan, S. Sayar, and S. Gunasekaran. Application of Peleg model to study water absorption in chickpea during. *Journal of Food Engineering*, 53:153–159, 2002.

[48] P. C. Vengaiah, R. K.Raigar, P. P.Srivastav, and G. C.Majumdar. Hydration characteristics of wheat grain. *Agricultural Engineering International: CIGR Journal*, 14:116–119, 2012.

[49] M. Kashiri, M. Kashaninejad, and N. Aghajani. Modeling water absorption of sorghum during soaking. *Latin American Applied Research*, 40:383–388, 2010.

[50] P. A. Sopade, E. S. Ajisegiri, and M. H. Badau. The use of Peleg's equation to model water absorption in some cereal grains during soaking. *Journal of Food Engineering*, 15:269–283, 1992.

[51] Philippos J. Pomonis and Eleni T. Tsaousi. Frenkel-halsey-hill equation, dimensionality of adsorption, and pore anisotropy. *Langmuir*, 25:9986–9994, 2009.

[52] W. D. Harkins and G. Jura. Surfaces of solids. XII. An absolute method for the determination of the area of a finely divided crystalline solid. *Journal of the American Chemical Society*, 66:1362–1366, 2009.

[53] M. Kruk, M. Jaroniec, and A. Sayari. Application of large pore MCM-41 molecular sieves to improve pore size analysis using nitrogen adsorption measurements. *Langmuir*, 13:6267–6273, 1997.

[54] Ellliott P. Barrett, Leslie G. Joyner, and Paul P. Halenda. The determination of pore volume and area distributions in porous substances. i. computations from nitrogen isotherms. *Journal of the American Chemical Society*, 73:373–380, 1951.

[55] Jhonny Villarroel-Rocha, Deicy Barrera, and Karim Sapag. Introducing a self-consistent test and the corresponding modification in the Barrett, Joyner and Halenda method for pore-size determination. *Microporous and Mesoporous Materials*, 20:68–78, 2014.

Appendix A: supplementary material

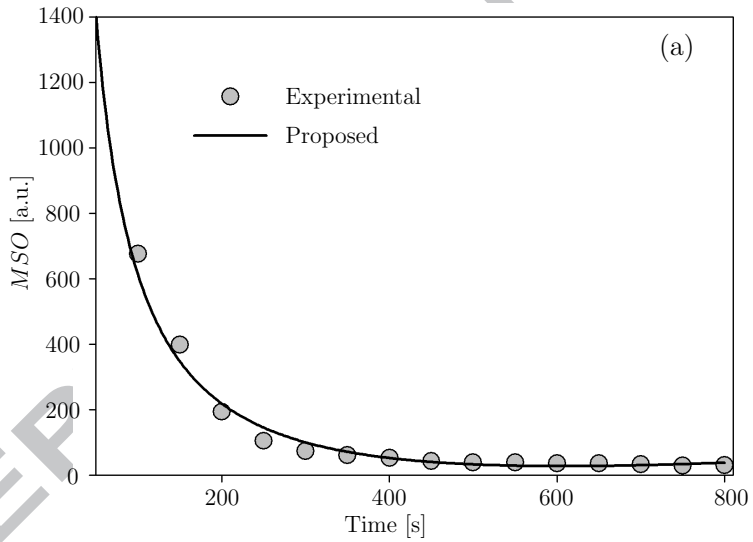

FIG. 9. *t*-plots for Z-HNO_3 of Hasley, Harkins and Jura and Harkins and Jura modified by Kruk models.

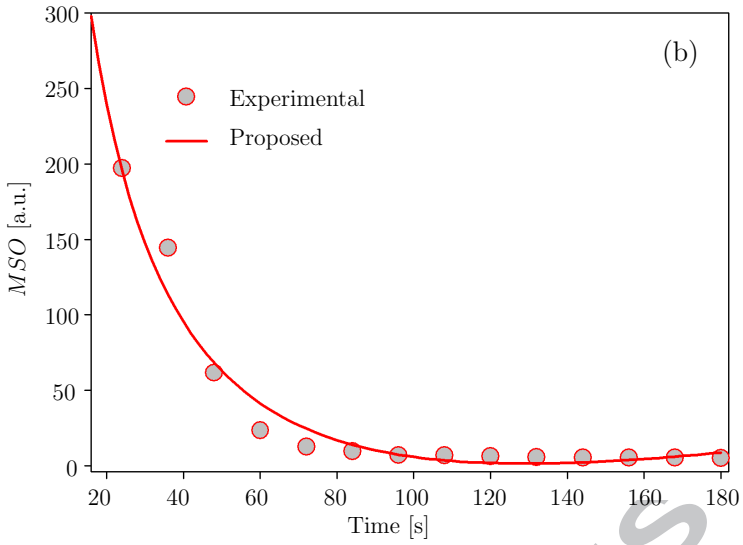

FIG. 10. t-plots for Z-NH_3 of Hasley, Harkins and Jura and Harkins and Jura modified by Kruk models.

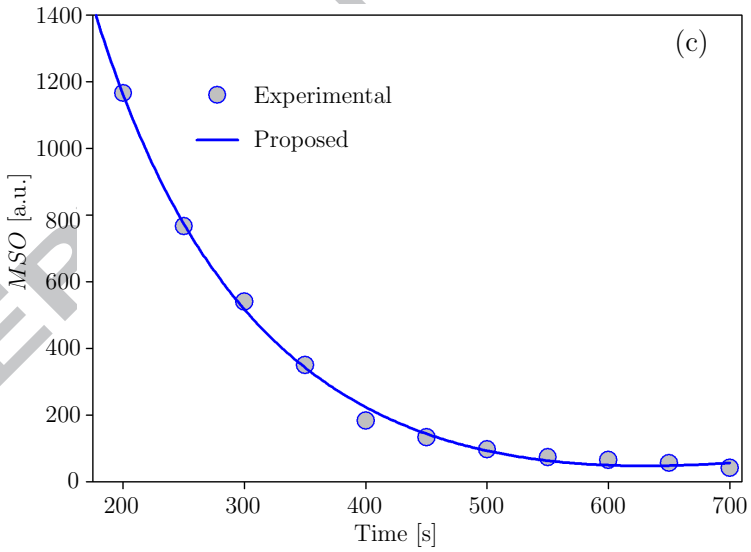

FIG. 11. t-plots for Z-250 of Hasley, Harkins and Jura and Harkins and Jura modified by Kruk models.

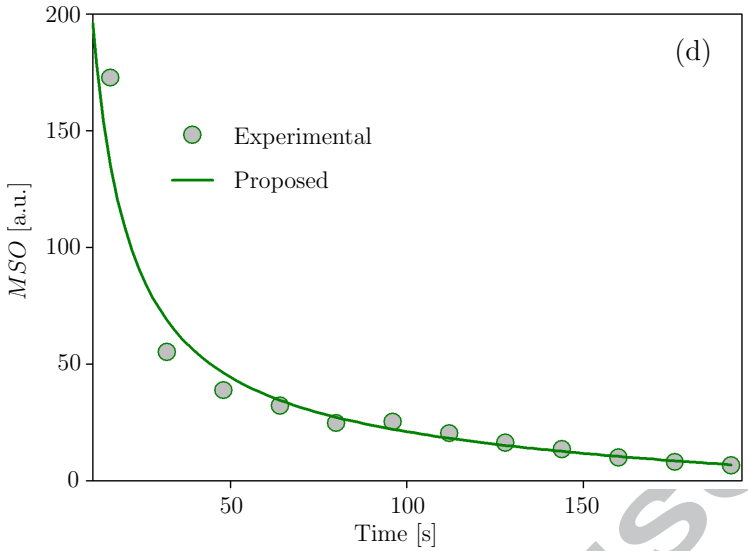

FIG. 12. t-plots for Z-500 of Hasley, Harkins and Jura and Harkins and Jura modified by Kruk models.

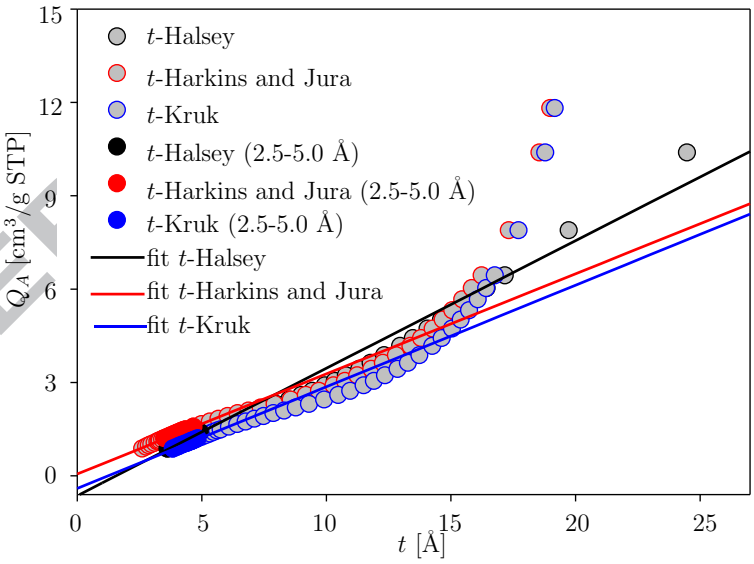

FIG. 13. Experimental values of the second order moment as a function of time and isotherm values adjusted by the different models for water adsorption of Z-HNO_3. DLS technique values in blue dots.

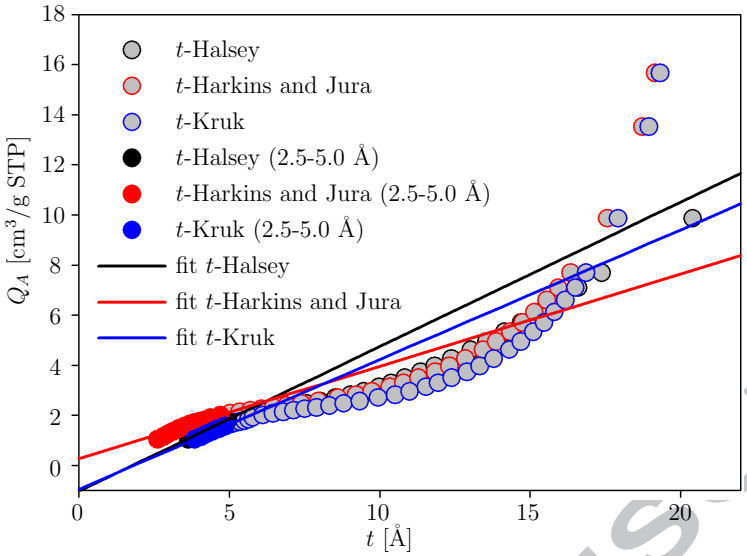

FIG. 14. Experimental values of the second order moment as a function of time and isotherm values adjusted by the different models for water adsorption of Z-NH_3. DLS technique values in blue dots.

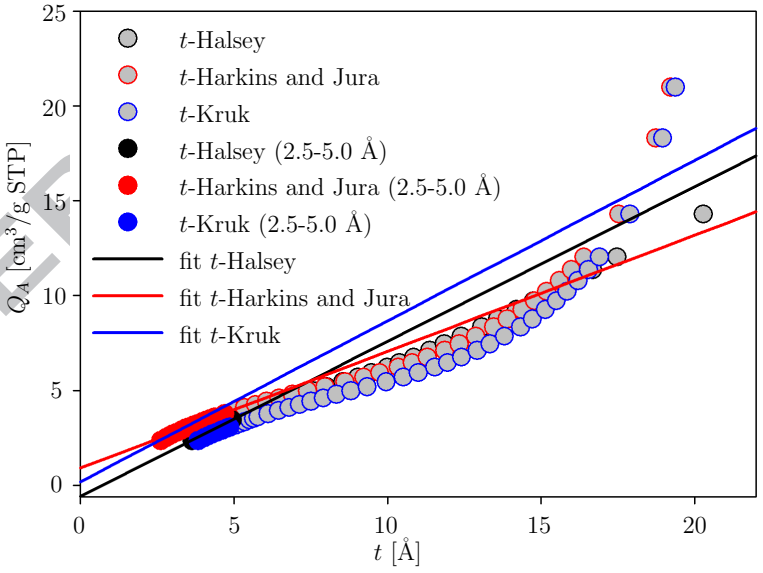

FIG. 15. Experimental values of the second order moment as a function of time and isotherm values adjusted by the different models for water adsorption of Z-250. DLS technique values in blue dots.

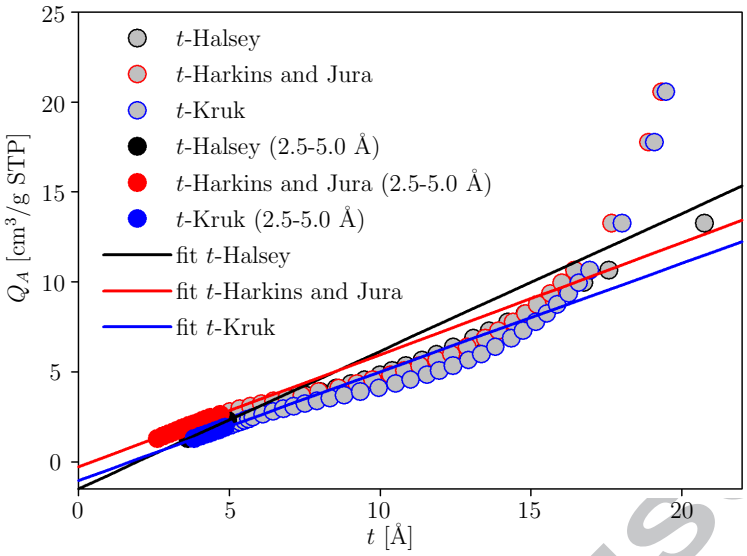

FIG. 16. Experimental values of the second order moment as a function of time and isotherm values adjusted by the different models for water adsorption of Z-500. DLS technique values in blue dots.

Highlights

New application of the Dynamic Laser Speckle (DLS) technique.

Hygroscopic capacity and specific surface area properties of pure and modified alumino-silicate.

DLS second order moment to experimentally determine the characteristic time "τ".

Surface area evaluation from the characteristic time "τ".

Conventional N_2 adsorption vs. characteristic time "τ" for specific surface area determination.

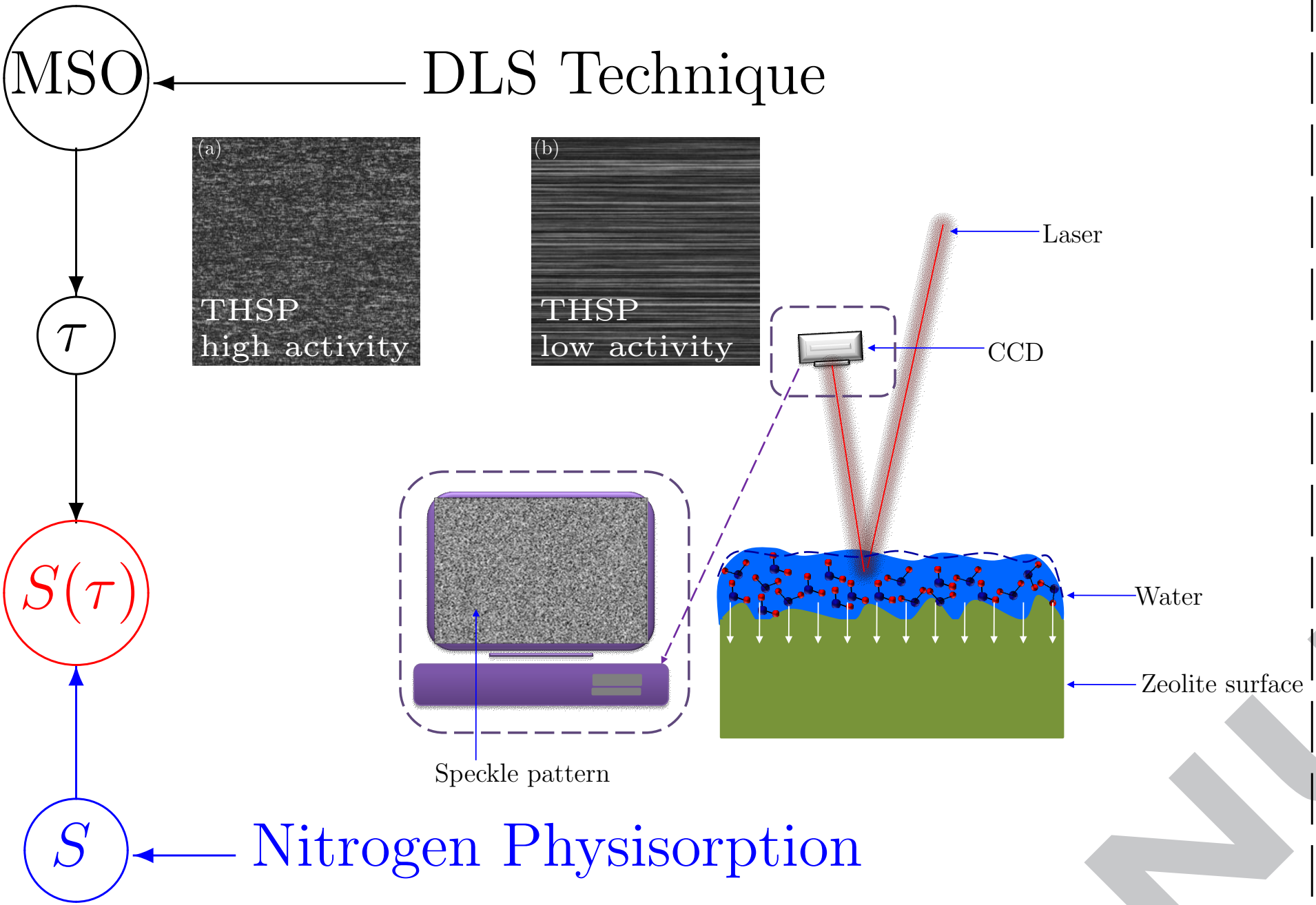
MSO
DLS Technique
(a)
THSP
high activity
(b)
THSP
low activity
τ
Laser
CCD
S(τ)
Water
Zeolite surface
Speckle pattern
S
Nitrogen Physisorption